

Synergic Comanipulation Despite Underactuated Robot

Anja Marx, Marie-Aude Vitrani, Benoît Herman, Răzvan Iordache, Serge Muller and Guillaume Morel

Abstract—The possibility to provide an adequate task assistance using underactuated robots for human-robot tool manipulation is investigated. This novel approach does not take into account any a priori knowledge about user depending parameters however optimizes the robot-user synergy, for instance during US breast examinations. Results show that the examination time can be reduced and a tendency for increasing scanning accuracy using underactuated robots.

I. COMANIPULATION FOR MEDICAL APPLICATIONS

Comanipulated devices are systems in which the robot and the user manipulate together the same tool. This paradigm is particularly interesting for medical applications. Indeed, unlike teleoperated systems, comanipulation devices allow the physician to remain with the patient, by directly handling the instruments that perform the gesture. In an ideal comanipulated system, the medical gesture is unchanged with the addition of a robot. The robot acts as a device providing active support to improve performance and to make the gesture safer. Comanipulation devices can be sorted in three categories, in function of the task that they perform.

A first task is to localize and calibrate the robot with respect to the patient. It is based on a typical force control law. If the desired effort applied by the robot is set to zero when the surgeon applies an effort onto the tool, the robot does not resist and so follows the user's gesture. In [1], a force compliance mode allows the surgeon to move the robot in order to locate centers of three pins implanted in a bone and to compute the appropriate location of the shape to be cut. In [2], a robotic system for skin harvesting is presented. When used in the manual mode, the surgeon can move the robot towards the initial pose on the skin, then towards the final pose to define the trajectory the robot must follow.

A second class of devices was developed to provide the surgeon with a better feeling of the tool-patient interaction. When the laparoscopic tool holder MC2E is force controlled with a zero desired force, the surgeon can feel the forces exerted on the tissues and organs without being corrupted by the trocar friction forces [3]. In [4], Taylor *et al.* proposed a steady-hand device for microsurgery. This device allows

scaling of interaction forces: forces applied by the surgeon on the eye are much lower than those felt by the surgeon.

This paper focuses on the third category that intends to guide the user by imposing kinematic constraints on the tool. To reach this goal, ancestors of “comanipulated” systems were presented in [5] for neurosurgery and spine surgery. In this paper, Cinquin *et al.* present two devices allowing to position a mechanical guide through which the surgeon introduces linear operative tools (e.g. drills). The limit of these systems is that the task must be divided into two successive actions—the first one is performed by the robot, and the second one by the surgeon while the robot remains inactive. As a consequence, only static constraints can be generated. Real-time adaptation is impossible. To overcome this, Schneider *et al.* propose a semi-passive device called “Passive Arm with Dynamic Constraints” (PADyC, [6]). Semi-passive means that any motion of the robot requires the action of the user. Its mechanical design enables to limit the motions of a tool according to a planned task. A geometrical zone is defined in which the surgeon can move freely. When moving out of the zone the surgeon feels forces applied by the robot to move him/her back inside the prescribed zone. This function of geometrical guidance is also proposed in [7] and [8]. Davies *et al.* present a robot for knee surgery named ACROBOT (Active Constraint ROBOT). The comanipulation does not result from a mechanical constraint but is provided by force control. The robot can be provided with regions of force constraints so that a flat or curved plane can be cut accurately into the bone to allow a prosthetic implant to be subsequently fitted. Furthermore, the robot can also be programmed to prevent any intrusion into adjacent regions, thus avoiding damage to ligaments. The basic idea behind active constraint control is to gradually increase the stiffness of the robot as it approaches the predefined boundary. The same principle is used to control the Surgicobot robot (based on a haptic device) which can be programmed with a desired apparent stiffness within a quite wide range, but without force sensors [8].

To the best of our knowledge, all systems within this latter class have sufficient actuated degrees of freedom (DOFs) to perform the task without a human user. However, imposing the desired kinematic constraints generally do not require so many actuators. In this paper, we study through an example the possibility to provide the adequate assistance for a comanipulation task with an underactuated robot. The immediate advantage is to have a more compact, less complex system at a lower cost. Careful attention must yet be paid to the system design to obtain the appropriate synergic behavior of the human-robot collaboration.

This work is partially funded by ANRT under CIFRE grant 247/2009.

A. Marx, M.-A. Vitrani, B. Herman and G. Morel are with UPMC Univ Paris 06, UMR 7222, ISIR, F-75005, Paris, France and CNRS, UMR 7222, ISIR, F-75005, Paris, France {marx, vitrani, morel}@isir.upmc.fr

A. Marx, R. Iordache and S. Muller are with GE Healthcare, Buc, France {anja.marx, razvan.iordache, serge.muller}@ge.com

B. Herman is now F.R.S.-FNRS Postdoctoral Researcher with Université catholique de Louvain, Center for Research in Mechatronics, B-1348 Louvain-la-Neuve, Belgium benoit.herman@uclouvain.be

The rest of the paper presents the particular medical context of breast cancer detection and the general comanipulation strategy in Section II. Then, in Section III, the chosen task and the proposed system are described. Finally, experimental results and discussions are detailed in Section IV.

II. NOVEL COMANIPULATION STRATEGY FOR US PROBE GUIDING

A. Clinical Context and Requirements

Digital breast tomosynthesis (DBT) is a new 3D X-ray imaging modality that overcomes one of the main limitations of the (2D) mammography, tissue overlapping. Ultrasound (US) imaging is the second most used imaging modality in breast cancer detection and diagnostic. Given the situation that a DBT scan shows multiple suspicious lesions within a patient's breast, the investigator usually calls for a supplementary manual US scan. This complementary examination aims at identifying tumors among the suspicious lesions. The big challenge of this additional examination is to find the previously identified suspicious zone in the US images of the now uncompressed breast. Note that during DBT scanning the patient's breast is compressed between a paddle and a detector, in order to avoid image noise due to patient movements like breathing. This is depicted in Fig. 1. However, for a successful US examination, it is usually necessary to decompress the patient's breast, because the compression paddles used in common DBT scans are not US compatible due to material characteristics. In addition to the difficult localization of the lesion, the mental matching between both image modalities gets more complicated because US examinations are mostly conducted hours or even days after the primary DBT scan, when a radiologist has analyzed and interpreted the DBT images.

A first way to make the US examination easier is to use novel US compatible compression paddles. This allows a US examination immediately after the DBT scan, while the breast remains compressed and so keeps its shape. DBT and US images show hence breast planes of the same breast pose, which facilitates the mental matching between both image modalities and the lesion localization. The radiologist task is

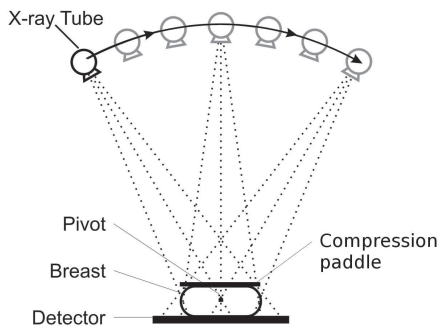


Fig. 1. DBT setup: The X-ray tube turns around its pivot point to scan the breast from different angles, which is compressed between the detector and a paddle.

then to find and scan the suspicious zone while maintaining contact between the probe and the paddle. This task has 4 DOFs, as shown in Fig. 2 and detailed in Section III below: two translations of the probe tip on the paddle, assumed to be planar, one rotation along the normal of the paddle surface, and a second rotation around the intersection line of the paddle surface and the US image plane.

From the physician point of view, the US scan remains complex even with this first improvement. He/she has still to mentally reconstruct the shape and 3D-location of the suspicious lesion from the DBT images, in order to position the probe. This mathematical and geometric computation could be performed easily by a computer. The deduced information could then be sent to a robot, that would guide the doctor towards the lesion with an expected increase of both speed and accuracy.

B. Purpose of Underactuation

The physician's arm and hand possess enough DOFs to move the probe while maintaining the contact with the paddle. The main difficulty to overcome is to locate the lesion with respect to the US plane. The most relevant pieces of information that would ease this location are the relative distance and the direction in which the probe should be moved to reach the target. This indication can be given by a force transmitted by the robot on the probe. A 3 DOFs haptic robot is therefore sufficient to provide the required assistance, although it is underactuated with respect to the 4 DOFs task—exerting a force on a point of the probe is clearly not sufficient to perform the task.

This force should be set to zero while the US plane intersects a lesion, or more generally a region of interest (ROI), in order to let the examiner translate and/or rotate the US probe freely. It must then increase progressively to indicate that he/she is moving away from the ROI, but with maintaining the possibility to scan regions outside the lesion.

An important requirement of the application is that the physician must be free to choose the 2D cross-section observed with the US-Probe to analyze the lesion. This means that he/she must be able to control either the position or the orientation of the probe (or both). The robot feedback

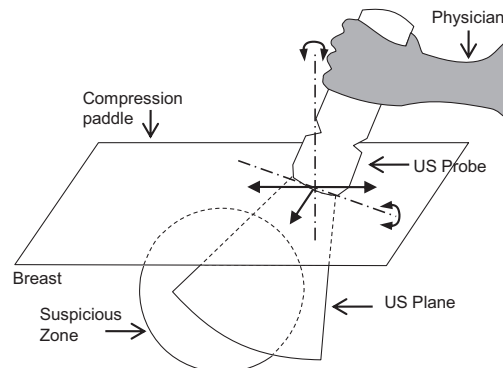


Fig. 2. Compressed breast scan with US Probe

should hence be given without any a priori knowledge of the user's strategy to bring back the US plane inside the ROI. Although it is not the only solution, underactuation can ensure this freedom of motion, under certain conditions to guarantee the human-robot-tool system stability. This is discussed in the next section, after the modeling of the US scan task and the computation of the required force.

III. TASK DESCRIPTION AND SYSTEM OVERVIEW

A. US Scan Modelling

Fig. 3 depicts the general model of the system. The ultrasound beam is assumed to be a plane denoted U which was experimentally validated in [9]. Furthermore, the paddle is said by the constructor to be a plane denoted π . In the next, the two following orthonormal coordinate frames are used :

- $\mathcal{F}_P = (P, \vec{x}_P, \vec{y}_P, \vec{z}_P)$, the frame attached to the probe with \vec{z}_P the vector normal to the ultrasound plane and P the origin of the US-ray.
- $\mathcal{F}_0 = (O, \vec{x}_0, \vec{y}_0, \vec{z}_0)$, the frame attached to the paddle with O a point belonging to the plane π and \vec{z}_0 the vector normal to it.

Furthermore, the ultrasound probe is handled by the human user at point H in such a way that $\vec{PH} = -\|\vec{PH}\|\vec{y}_P$. The robot can apply a force on the probe at point T , defined as $\vec{PT} = -\|\vec{PT}\|\vec{y}_P$. The point of the suspicious lesion which minimizes the distance to the ultrasound plane U is denoted I . Its projection on the ultrasound plane is denoted I_U .

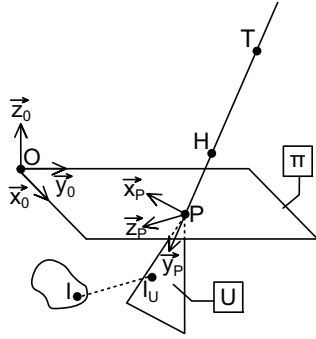


Fig. 3. Geometrical modelling

B. Computation of Desired Force

In most surgical applications, the tool (e.g. saw, drill) must be kept inside a prescribed zone. When it approaches the border of the “free motion” zone, a common comanipulation scheme will increase rapidly the force to reach a value that locks any further motion towards the border. As stated above, in the present application, the doctor might want to scan regions around the ROI. Consequently, the robot should not prevent the user from moving out of the ROI. It should only apply a force that increases proportionally with the distance $\vec{d} = \vec{II}_U$ between the US plane and the target. This force

$$\vec{F} = k\vec{d} \quad (1)$$

simulates the behavior of an ideal spring with a stiffness k .

The vertical component of this force along \vec{z}_0 should be set to zero in order to avoid any disturbance on the contact constraint. Therefore,

$$\vec{F} = k \left[\vec{d} - (\vec{d} \cdot \vec{z}_0) \vec{z}_0 \right]. \quad (2)$$

This spring force should also be damped to maintain stability even under a rapid change of the distance \vec{d} . This can occur in configurations where a small rotation of the probe creates a large variation of the distance. Thus, the force becomes

$$\vec{F} = k \left[\vec{d} - (\vec{d} \cdot \vec{z}_0) \vec{z}_0 \right] + c \frac{\Delta \vec{d}}{\Delta t}, \quad (3)$$

where c is the damping coefficient.

Moreover, a second damping factor was included to avoid end-effector oscillations. This is required by technical limitations of the robot chosen for the experimental setup (see Section IV below). It is proportional to the end-effector's velocity $\vec{v}_T = \frac{\Delta \vec{OT}}{\Delta t}$ computed over the same period Δt :

$$\vec{F} = k \left[\vec{d} - (\vec{d} \cdot \vec{z}_0) \vec{z}_0 \right] + c \frac{\Delta \vec{d}}{\Delta t} + c_T \frac{\Delta \vec{OT}}{\Delta t}. \quad (4)$$

Finally, a constant balancing force was added to compensate the US probe and robot arm weight. This avoids the user to carry a too heavy weight and prevents the US probe from falling down once the user releases the probe. The final force is then

$$\vec{F} = k \left[\vec{d} - (\vec{d} \cdot \vec{z}_0) \vec{z}_0 \right] + c \frac{\Delta \vec{d}}{\Delta t} + c_T \frac{\Delta \vec{OT}}{\Delta t} + mg\vec{z}_0, \quad (5)$$

where the mass m was estimated manually according to the best haptic sensation.

C. Robot-Probe Interaction

One can state two possible configurations for the relative placement of the hand and robot end-effector on the probe. The user might grasp the probe *above* the robot end-effector tip (see Fig. 4) or *below* (see Fig. 5). The second solution, called hereafter “direct probe grasp”, seems to be more suitable because the physician can still grasp the probe at its bottom end with few interference from the robot. Unfortunately, this leads to an unstable behavior, contrary to “end-effector grasp” as explained below.

1) *Direct Probe Grasp*: In case of directly grasping the probe, the user's stiffness requires two different control laws to accomplish the scanning task around a ROI.

Stiff Grasp: The user's hand is tightened and does not permit any probe movement or sliding within the hand. To change the probe's pose to a desired position the user follows the direction indicated by the robot. Hence a force in the direction of the desired probe position, towards the center of the ROI (POI) I , is applied. Fig. 6 sketches the geometrical model for this case. H represents the user's hand, P the origin of the US plane and T the robot end-effector tip. To achieve a moving of the US plane U for a stiff user grasp, a force in f_{dir} has to be applied in T . Note, that due to the robot architecture, it can only apply forces in T . As the

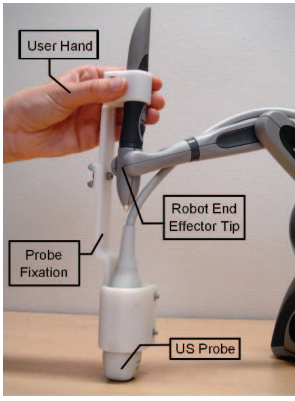


Fig. 4. “end-effector grasp”: tool handling with hand above robot end-effector tip.

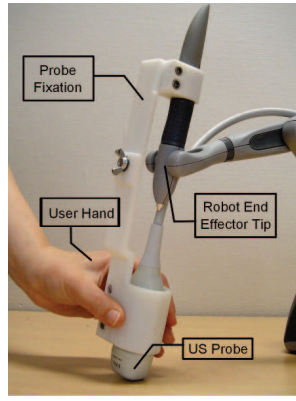


Fig. 5. “direct probe grasp”: tool handling with hand below robot end-effector tip.

probe is rigidly attached to T and the user has a stiff grasp, that means follows the robot indications, f_{dir} causes a hand movement towards I . This results in a new position for T and P , T' and P' respectively, where U intersects I .

Soft Grasp: The user’s hand is relaxed and permits the probe to change its orientation within the hand when the robot applies a force. Hence, once the robot moves, the human grasp provokes a pivot point of the hang-up at the height of the fingers. This means, the probe orientation changes with every end-effector shift. Fig. 7 displays the geometrical representation for this case. To achieve an intersection of the US plane and the POI, the robot has to apply a force f_{dir} in the opposite direction as for a stiff grasp. This is due to the fact that H acts as a rotation point due to the soft grasp.

One can state two different robot control laws for a direct probe handle which differ only in a sign. The choice of the control law is hence highly dependent on the user’s stiffness, i.e. its soft or stiff grasp. As this is not a priori known, the wrong choice of the force direction can result in an unstable system which is not appropriate for any system.

2) *End-effector Grasp*: When manipulating the imaging tool above the robot end-effector, one can note that in both cases the direction of the applied force remains the same.

Stiff Grasp: Similar to the case described above, a stiff

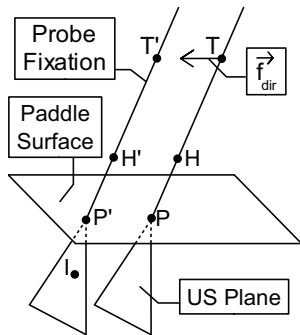


Fig. 6. “direct probe grasp”: probe orientation and position for stiff grasps.

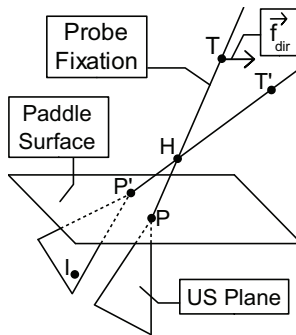


Fig. 7. “direct probe grasp”: probe orientation and position for soft grasps.

grasp does not permit any end-effector movement or sliding within the hand. The user keeps the end-effector tight within the hand and follows the direction indicated by the robot. As the probe is rigidly attached to the end-effector, its pose changes with any end-effector movement. To approach the US plane to I , a force is hence applied in T in the direction of the desired probe position. Fig. 8 sketches this principle.

Soft Grasp: The user softly holds the end-effector and permits it to slide within the hand when the robot applies a force. Hence, once the robot moves, the human grasp provokes a pivot point at the fingers level. This means, the probe orientation is changed whereas the hand position remains relatively stable. To sight a POI, the robot applies a force in direction of the POI to change the probe orientation. Fig. 9 displays the geometrical model for this case.

This analysis for a direct end-effector grasp shows that regardless of the user’s stiffness the returned force direction remains the same to successfully accomplish the scanning task. This is the main reason why we chose to implement this solution. Furthermore, the returned force indicates the user a problematic probe state, i.e. a too large distance to the POI or ROI, and at the same time proposes a solution to better perform the actual task without restricting the user movement. As described in Section II, this behavior was one of the main requirements for this haptic system.

IV. EXPERIMENTAL VALIDATION

A. Setup

We chose to use a PHANToM Omni robot (SensAble Technologies, Inc., Woburn, MA). It is a commercially available 6 DOFs haptic robot. Three DOFs are actuated to position a point of the end-effector. The three other DOFs (orientation of the end-effector with respect to the robot base) are not actuated. This robot is designed to produce a force feedback at its end-effector tip. The PHANToM Omni robot hence satisfies the demand of having less steerable degrees than would be needed to automatically execute the task. In addition it is easy to handle and has low friction.

To manipulate the US probe, a probe fixation was designed to rigidly mount the probe on the robot end-effector. This implies that any force applied on the robot end-effector has

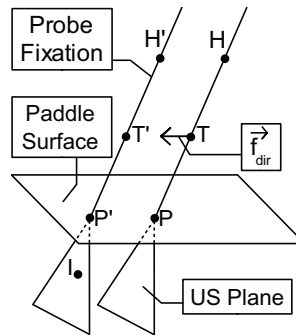


Fig. 8. “end-effector grasp”: probe orientation and position for stiff grasps.

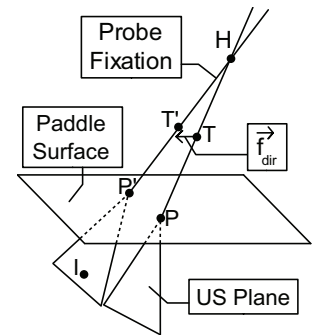


Fig. 9. “end-effector grasp”: probe orientation and position for soft grasps.

TABLE I
RESULTS FOR EXPERIMENTS USING THE ROBOT IN PASSIVE AND ACTIVE MODES

	Passive robot			Active robot		
	Intuition Mean (SD)	Soft grasp Mean (SD)	Firm grasp Mean (SD)	Intuition Mean (SD)	Soft grasp Mean (SD)	Firm grasp Mean (SD)
Completion time [s]	7.29 (2.42)	8.11 (4.34)	7.48 (3.05)	6.04 (1.84)	6.85 (2.68)	5.54 (1.75)
Approaching time [%]	18.26 (6.52)	21.22 (0.04)	22.02(8.50)	24.05 (13.47)	26.78 (11.74)	23.29 (9.71)
Mean distance to ROI [mm]	8.12 (7.02)	6.66 (7.55)	7.38 (6.19)	7.34 (5.21)	5.29 (6.93)	4.99 (3.31)
Max. distance to ROI [mm]	32.20 (21.10)	38.08 (19.94)	34.82 (24.81)	21.14 (7.65)	30.72 (18.65)	25.93 (8.56)
Scanning frames inside ROI [%]	49.35 (15.69)	54.30 (22.11)	54.62 (25.22)	58.78 (17.42)	54.59 (19.12)	53.06 (6.81)

better performances using an active robot support, 59 % compared to 49 %. Standard deviation tends also to decrease for the active robot mode.

It is obvious that using a 3D visual interface introduces a bias—for both active and passive modes—as it provides the user with 3D information about the scanned object and the actual plane position. Usually during the current clinical practice only 2D visual feedback is given by displaying the actual US image and a 3D slice reconstruction of the patient's breast. Investigators normally only have a vague idea about the lesion location. It is hence likely that results for the scanning task with neither 3D visual feedback nor active robot support are even worse. Indeed, the measured improvements can directly be attributed to the proposed robotic assistance, but further work should be done to quantify the influence of an improved visual feedback.

Finally, as mentioned in Section I, the medical gesture should remain unchanged in an ideal comanipulation system. Due to stability problems identified in Section III, we were forced to modify the probe grasp. This might have an impact on the acceptability of the comanipulation system. Future work is planned to overcome those difficulties.

V. CONCLUSIONS

This paper demonstrates the possibility to provide an adequate task assistance using underactuated robots for human-robot tool comanipulation. The example studied leans on US scans examinations consecutive to DBT scans for early breast cancer detection.

In our approach, a robot comanipulates the hand-held US probe and is programmed to assist the user in scanning a ROI previously identified thanks to the DBT scan. It indicates when the US plane is too far away from the ROI and helps to come back inside it. Both indication and assistance to execute the task are done by applying a simple force on the US probe by the robot end-effector.

We rigidly attached a US probe to a PHANToM Omni robot for the implementation of this novel system. The probe pose is hence influenced by the user grasp and the robot feedback. Additional 3D visual feedback was given by displaying a virtual 3D scene of the ROI and the US plane.

The user performances using this novel system to conduct a scanning task were compared to data on usual US scanning without active robot support but with 3D visual feedback. Experimental results demonstrate the successful integration

of a robot to an imaging system to improve task accuracy and completion time regardless of the user grasping strategy. For intuitive probe handling, results for maximal plane-ROI distance as well as percentage of frames with plane-ROI intersection could be markedly improved. Furthermore, completion time decreases with active comanipulation.

After these first encouraging results, a realistic test setup has to be conceived to evaluate further implementation possibilities and minimal robot requirements. Therefore the use of a higher-performance robot having a larger working space and stronger force feedback capacities is considered. The next important step is to improve the robot-probe attachment to provide the user a standard probe handle, i.e. approach the robot end effector a maximum towards the probe tip. Finally, US and DBT data have to be introduced directly to the test setup to estimate the visual bias on user performances and a larger validation series has to be performed.

REFERENCES

- [1] R. Taylor, B. Mittelstadt, H. Paul, W. Hanson, P. Kazanzides, J. Zuhars, B. Williamson, B. Musits, E. Glassman, and W. Bargar, "An image-directed robotic system for precise orthopaedic surgery," *IEEE Trans. Robot. Automat.*, vol. 10, no. 3, pp. 261–275, June 1994.
- [2] E. Dombre, G. Duchemin, P. Poinet, and F. Pierrot, "Dermarob: A safe robot for reconstructive surgery," *IEEE Trans. Robot. Automat.*, vol. 19, no. 5, pp. 876–884, Oct. 2003.
- [3] N. Zemiti, T. Ortmaier, M.-A. Vitrani, and G. Morel, "A force controlled laparoscopic surgical robot without distal force sensing," in *Experimental Robotics IX*, ser. Springer Tracts in Advanced Robotics, M. Ang and O. Khatib, Eds. Springer Berlin / Heidelberg, 2006, vol. 21, pp. 153–164.
- [4] R. Taylor, P. Jensen, L. Whitcomb, A. Barnes, R. Kumar, D. Stoianovici, P. Gupta, Z. Wang, E. Dejuan, and L. Kavoussi, "A steady-hand robotic system for microsurgical augmentation," *International Journal of Robotics Research*, vol. 18, no. 12, pp. 1201–1210, 1999.
- [5] P. Cinquin, S. Lavalée, and J. Troccaz, "Igor : Image guided operating robot. methodology, applications," in *Proc. IEEE International Conference of the Engineering in Medicine and Biology Society (EMBS'92)*, Nov. 1992, pp. 1048–1049.
- [6] O. Schneider, J. Troccaz, O. Chavanon, and D. Blin, "Padyc: a synergistic robot for cardiac puncturing," in *Proc. IEEE International Conference on Robotics and Automation(ICRA'00)*, Apr. 2000, pp. 2883–2888.
- [7] B. Davies, K. Fan, R. Hibberd, M. Jakopec, and S. Harris, "A mechatronic based robotic system for knee surgery," in *Proc. IASTED International Conference on Intelligent Information Systems (IIS'97)*, Dec. 1997, pp. 48–52.
- [8] E. Bonneau, F. Taha, P. Gravez, and S. Lamy, "Surgicobot: Surgical gesture assistance cobot for maxillo-facial interventions," *Perspectives in Image-Guided Surgery*, pp. 353–360, Mar. 2004.
- [9] M.-A. Vitrani and G. Morel, "Hand-eye self-calibration of an ultrasound image-based robotic system," in *Proc. IEEE/RSJ International Conference on Intelligent Robots and Systems (IROS'08)*, 2008, pp. 1179–1185.